Design of a Radio Frequency Compensation System, using the Electrical Characterisation of a Multi-Transducer Acousto-Optical Tunable Filter

J. Vanhamel, Samuel Dupont, Jean-Claude Kastelik, E. Dekemper

DOI: 10.61782/fa.2023.0379

forum acusticum 2023

DESIGN OF A RADIO FREQUENCY COMPENSATION SYSTEM, USING THE ELECTRICAL CHARACTERISATION OF A MULTI-TRANSDUCER ACOUSTO-OPTICAL TUNABLE FILTER

Jurgen Vanhamel[1,2*] **Samuel Dupont**[3] **Jean-Claude Kastelik**[3]
Emmanuel Dekemper[4]

[1] TU Delft - Faculty of Aerospace Engineering, Kluyverweg 1, 2629 HS Delft, The Netherlands
[2] Electronic Circuits and Systems, KU Leuven, Kleinhoefstraat 4, 2440 Geel, Belgium
[3] l'Université Polytechnique Hauts-de-France (UPHF), IEMN – Campus Mont Huy – Cedex 9, 59313 Valenciennes, France
[4] Royal Belgian Institute for Space Aeronomy (BIRA-IASB), Ringlaan 3, 1180 Brussels, Belgium

ABSTRACT

Acousto-Optical Tunable Filters (AOTFs) make use of the interaction between sound and light. To generate an ultrasound diffraction grating, a Radio-Frequency (RF) signal is applied to a piezoelectric transducer. The optical pass band can be controlled by adapting the properties of this transducer and the RF-signal. To achieve more precise control of the optical spectral bandwidth, we propose to use a multi-electrode array, consisting of five consecutive transducers. The Voltage Standing Wave Ratio (VSWR) is then used to evaluate the efficiency of the coupling between the RF-signal applied to the transducer and the acousto-optical crystal. A higher VSWR indicates that more power is being reflected back and less is being absorbed by the transducer, which in turn results in a decrease in optical performance.
The aim of this paper is to develop an RF driving system capable of compensating for the VSWR behavior, linked to the individual impedance matching network of each transducer. For this, the five transducer setups were electrically characterized. These measurements allow the development of an RF power compensation system, leading to an increase of applied power at the level of each transducer. Hence, the absorbed power at transducer level increases, resulting in improved optical diffraction efficiency.

Keywords: *AOTF, RF-steering, compensation, VSWR.*

1. INTRODUCTION

Acousto-Optic Tunable Filters (AOTFs) use acoustic waves to control the diffraction of light entering the transparent crystal. A wide range of applications can be covered with these devices, including spectroscopy, telecommunications and tracking technology for space applications [1, 2, 3]. The setup of AOTFs allows for a fast, highly efficient and precise control over the spectral properties of light. This makes AOTFs an attractive option for a variety of applications where optical filtering is required. AOTFs applied in spectroscopy can be used to select or block specific optical wavelengths [4]. This allows for a precise selection and measurement of spectral lines, which can provide information about the chemical composition of a specific sample.
In order to activate these AOTFs and to control the diffraction of light at a specific optical wavelength, a transducer is mounted to the side of a transparent crystal (made of TeO_2, quartz or another material). This allows the conversion of Radio-Frequency (RF) signals of a specific frequency and power into soundwaves [5]. To initiate this, a

[*] ***Corresponding author***: j.a.m.vanhamel@tudelft.nl

piezo-electric element is used, expanding and contracting as a response to the applied RF signal. Mostly, the RF frequency range is limited to one octave in order to avoid harmonic signals and spurs to occur in the RF spectrum. These anomalies can create additional soundwaves inside the crystal which disturb the interaction between sound and light.

In order to increase the resolution of the optical transmission curve of the AOTF, a multiple transducer setup can be used. Consequently, a variation of the spectral resolution can be obtained [6], creating a multi-purpose device.

Each transducer comes with a specific designed electrical impedance matching network, responsible for the high efficient conversion of RF energy into soundwaves [7]. If this network is not fully matched to 50 Ohm over the applied frequency range, the conversion of RF energy into soundwaves cannot be done in the most optimal way and RF amplitude inhomogeneity exists. Typically, a part of the applied RF energy is reflected back to the RF chain. The combination of each transducer and its individual electrical impedance matching network is called the transducer setup (see dashed line in Fig. 1). Additionally, since the transducer sections have different properties, the phase characteristics of each transducer setup differ as well. These differences can emit acoustic waves with different phase delays which can influence the AOTF performance in a significant way [8].

The aim of this paper is to analyze and characterize each transducer setup (combination transducer and electrical impedance matching network) of the multi-transducer AOTF in relation to the RF amplitude inhomogeneity. Based on the outcome, a power compensation system is designed in order to compensate for the reflected RF energy. Subsequently, the amount of power at transducer level can be increased significantly, obtaining a higher optical efficiency.

2. RF CONVERSION AND CHARACTERIZATION PRINCIPLE

The working principle of an AOTF is based on the interaction between soundwaves produced within a birefringent crystal (e.g. made of TeO_2) and incoming light. When the Bragg matching condition is satisfied, two beams of first-order diffracted light are emitted at the crystal's output [5] (Fig. 1). The transducer attached to the crystal allows the conversion of RF energy into soundwaves. In standard AOTF devices, only one transducer setup is used. In this work a multi-transducer setup is discussed.

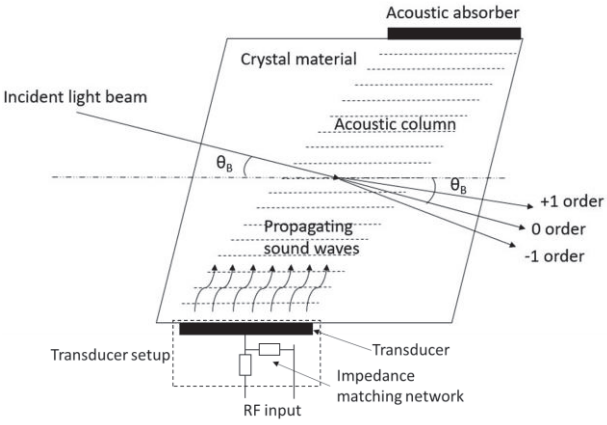

Figure 1. AOTF working principle. Adapted with permission from reference [7] by OSA Publishing

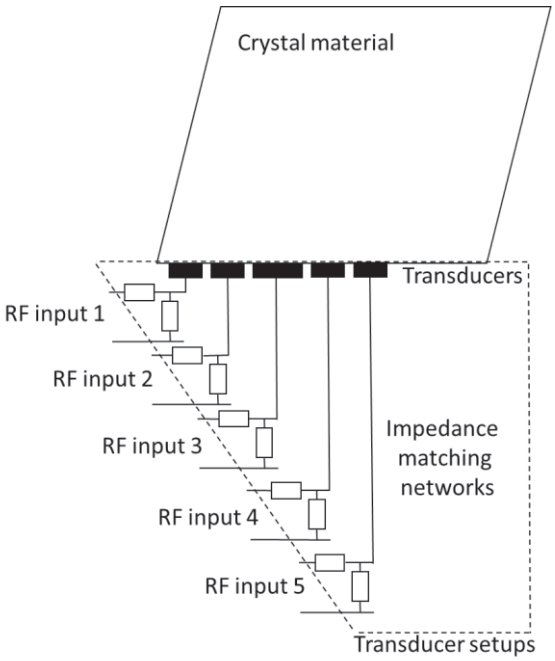

Figure 2. VIS AOTF transducer setups (= transducer – impedance matching network combinations).

2.1 Impedance network - transducer combination

In this multi-transducer setup, each of the five transducers has a specific RF impedance behavior as a function of the applied frequency. In front of each transducer an individual

electric impedance matching network is used in order to apply the RF energy in the most optimal way to the transducer (Fig. 2). Typically, these networks are designed to behave as a 50 Ohm resistor at a limited band around one specific frequency. In the transducer setup, this range has to be wider (around one octave) in order to assure a broad optical range [9, 10]. Consequently, the conversion of RF energy into soundwaves cannot be done at the most optimal conversion rate. Typically around a quarter of the applied RF energy is not reaching the transducer in the usable frequency range [10].

2.2 Multi-transducer characterization

The use of multi-transducer setups enables the increase in resolution of the optical transmission curve [6]. This enables a variation of the spectral bandwidth as function of the wavelength, compared to a single transducer setup [6]. In this paper, the authors examined a multi-transducer Visible (VIS) AOTF of the company AA Opto Electronic, consisting of five separate transducers, each of a specific dimension, and each having a dedicated electrical impedance matching network (Fig. 3). The width of the transducer determines the acoustic column inside the crystal.

Figure 3. Multi-transducer VIS AOTF obtained at AA Opto Electronic.

In order to have a detailed view on how this multi-transducer and accompanying electric impedance matching networks behave, the Voltage Standing Wave Ratio (VSWR) is measured. This parameter reveals the conversion behavior of each electric impedance network and allows a detailed analysis of the electrical circuit [7].

The aim of this work is to characterize the VSWR of each individual transducer-impedance network combination. Based on this value, a power compensation system is designed in order to compensate for the reflected RF energy occurring if the impedance is not matched correctly to 50 Ohm.

3. OPTIMAL RF DRIVING SYSTEM

The used VIS AOTF is composed of five transducers, mounted adjoining. The middle transducer has a width of 3 mm, while the other four each have a width of 2 mm. Hence, a symmetrical setup occurs around the central 3 mm transducer (Fig. 2). Each transducer has his specific electric impedance matching network and accompanying RF input connector (Fig. 2 and 3).

3.1 Experimental setup

To characterize the electric impedance matching network of each transducer setup, the HP4195A Vector Network Analyzer (VNA) is used in combination with the Rohde & Schwarz ZCAN 800.8515.52 calibration kit, for measuring the S11 parameter. The experimental setup is shown in Fig. 4. For each measurement, the calibration kit is used in order to have a fully calibrated setup (dashed line toward the calibration kit in Fig. 4). Additionally, each transducer setup is characterized one by one (dashed lines towards the five RF inputs of the VIS AOTF).

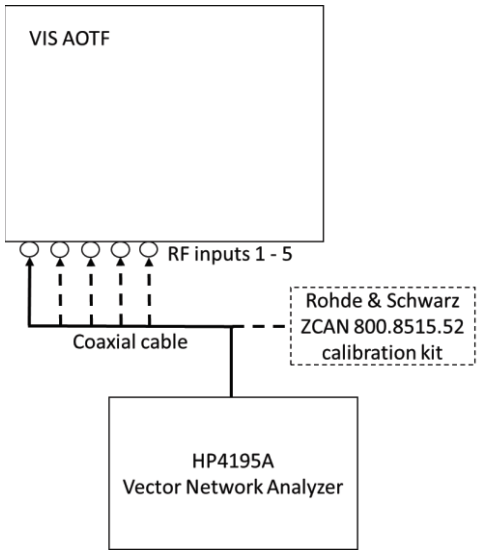

Figure 4. Test setup in order to characterize the different transducer setups of the VIS AOTF.

3.2 Measurement results

Measurements are carried out at different frequencies, starting at 30 MHz up to 110 MHz. In steps of 200 kHz, the S11 parameter is measured using the VNA. This range is broader than the scope prescribed by the manufacturer (54 – 88 MHz). With this parameter, the VSWR can be calculated, using Eqn. 1 [11], in which Γ is the reflection coefficient, using the S11 parameter.

$$VSWR = \frac{(1 + |\Gamma|)}{(1 - |\Gamma|)} \quad (1)$$

This VSWR value is calculated for all five transducer setups of the VIS AOTF. The results are shown in Fig. 5.

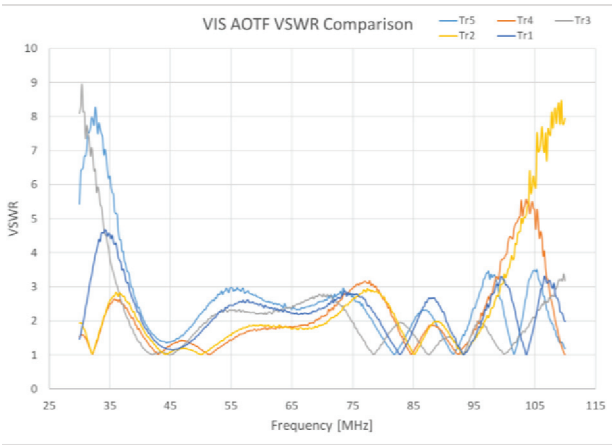

Figure 5. VSWR comparison graph for all five transducer setups. Tr1 = leftmost transducer (2 mm), Tr2 = second from the left transducer (2 mm), Tr3 = middle transducer (3 mm), Tr4 = second from the right transducer (2 mm), Tr5 = right transducer (2 mm).

Based on the results, it is shown that the usable frequency range in which this VIS AOTF is practically applicable is limited to 54 – 88 MHz, as specified by the manufacturer. In this region, the VSWR has a rather low value (on average around 2.5:1), which indicates only a limited amount of power is reflected.
What also can be noticed is the slight difference in VSWR in the optimal frequency range (54 – 88 MHz) between the different transducer setups. There is a symmetry between transducer setup 1 and 5, and between transducer setup 2 and 4.

3.3 Compensation principle and system

Based on the different VSWR graphs for the five transducer setups, the impact factor of the Mismatch Loss (ML) is calculated using Eqn. 2 [11].

$$ML\,[dB] = -10\,log\left[1 - \left(\frac{VSWR - 1}{VSWR + 1}\right)^2\right] \quad (2)$$

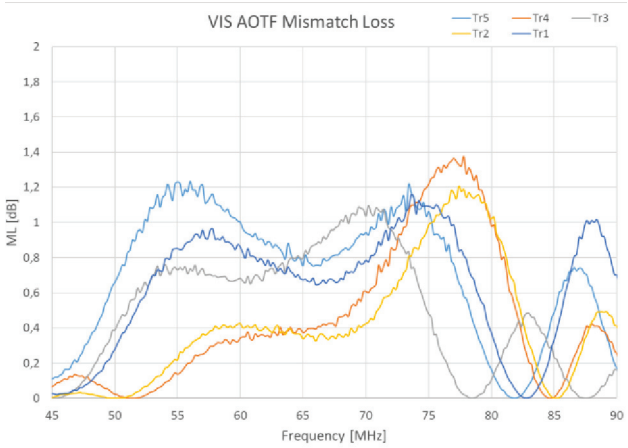

Figure 6. Mismatch Loss (in dB) for all five transducer setups in the applicable RF frequency range. Tr1 = leftmost transducer (2 mm), Tr2 = second from the left transducer (2 mm), Tr3 = middle transducer (3 mm), Tr4 = second from the right transducer (2 mm), Tr5 = right transducer (2 mm).

The ML indicates how much power is reflected back into the RF driving system. In Fig. 6, the amount of reflected power (in dB) is given as a function of the frequency for all five transducer setups (Tr1 – 5). The graph indicates that different RF driving power is needed for each transducer setup, depending on the applied frequency. Based on these values, the nominal applied RF power has to be increased by the indicated amount of dB, in order to compensate for the reflected power loss in each transducer setup. By doing so, the actual power applied at transducer level is higher and the optical diffraction efficiency of the AOTF increases. If this compensation is done for each ML at each frequency, a full RF power loss compensation system is possible. In practice this means that for transducer setup 1 (Tr1 in Fig. 6), a frequency dependent RF driving compensation power is needed between 0 and 1.1 dB on top of the nominal RF power. As an example, at 75 MHz, a compensation of 1.1 dB is needed for the ML (Fig. 6). This means that instead of applying a nominal RF power of for example 20 dBm (=

100 mW), 20 dBm + 1.1 dB = 21.1 dBm (= 129 mW) should be applied to the transducer setup. This total power, which is the sum of the nominal applied RF power and the RF driving compensation power, indicates a significant difference compared to the nominal applied RF power. The latter clearly does not take into account the ML.

Again, Fig. 6 shows the symmetry between transducer setup 1 and 5, as well as between transducer setup 2 and 4. The ML behavior for those paired transducer setups is comparable.

Based on the graph of Fig. 6, an RF power compensation system can be designed, using different techniques such as an analog RF driving setup using a Phase-Locked-Loop (PLL) [12], or a fully digital approach such as a Direct Digital Synthesis (DDS) driver [13]. A possible setup is shown in Fig. 7. The setup shows how the compensation of the ML should be taken into account. For each transducer setup, the additional amount of power varies, depending on the used RF frequency (see Fig. 6). This frequency dependent variation lays between 0 dB and 1.4 dB. This extra power needs to be added to the nominal RF power in order to achieve the optimal diffraction efficiency. This optimal nominal RF power ($P_{OPTIMAL}$) is calculated using Eqn. 3 [14]:

$$P_{OPTIMAL} \cong \frac{\lambda^2 H}{2\,L\,M_2} \tag{3}$$

in which L and H are the physical length and height of the transducer, λ is the wavelength of the optical light beam entering the crystal, and M_2 the figure of merit depending on the material of the used crystal [14].

Design of such a RF driving compensation system is part of future work.

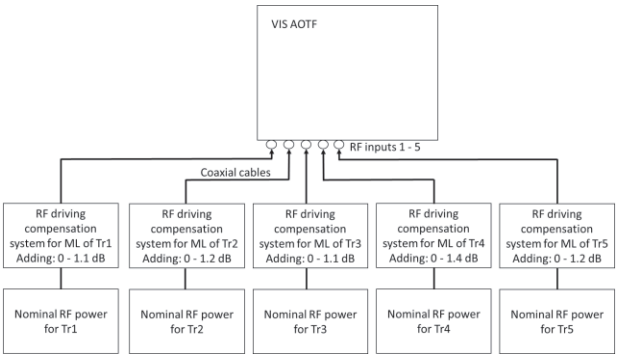

Figure 7. RF driving system to compensate for the ML of each transducer setup.

4. CONCLUSIONS

In this work, a multiple transducer VIS AOTF of AA Opto Electronic was electrically characterized. The device consists of five transducers, each having their dedicated impedance matching network. The latter does not consistently achieve an exact 50 Ohm match across the entire frequency range of the VIS AOTF. Consequently, the conversion of RF energy into soundwaves cannot be done in the most optimal way. In order to compensate for the impedance mismatch, each transducer setup was first characterized by obtaining the S11-parameter. The latter was converted into the VSWR, and additionally used to calculate the ML. This parameter indicates the amount of power which is reflected back into the RF chain. An RF driving compensation system for ML was proposed in order to optimize the diffraction efficiency of the VIS AOTF from an RF amplitude point-of-view. This system combines the nominal applied RF power with the RF driving compensation power, based on the ML. The concrete practical implementation of this system is part of future work.

5. ACKNOWLEDGMENTS

The authors would like to thank l'Université Polytechnique Hauts-de-France (UPHF), the Delft University of Technology (TU Delft) and the Royal Belgian Institute for Space Aeronomy (BIRA-IASB) to accommodate this collaboration and experimental work.

6. REFERENCES

[1] E. Dekemper, J. Vanhamel, B. Van Opstal, and D. Fussen: "The AOTF-based NO_2 camera," *Atmos. Meas. Tech.*, vol. 9, pp. 6025–6034, 2016.

[2] J.R. Kerr, P.J. Titterton, A.R. Kraemer, and C.R. Cooke, "Atmospheric Optical Communications Systems" in *Proceedings of the IEEE*, vol. 58, no. 10, pp. 1691-1709, 1970.

[3] E. Swanson and V. Chan: "Heterodyne Spatial Tracking System for Optical Space Communication," *IEEE Transactions on Communications*, vol. 34, no. 2, pp. 118-126, 1986.

[4] E. Dekemper, N. Loodts, B. Van Opstal, J. Maes, F. Vanhellemont, N. Mateshvili, G. Franssens, D. Pieroux, C. Bingen, C. Robert, L. Devos, L. Aballea, and D. Fussen, "Tunable acousto-optic spectral imager for atmospheric composition measurements in the

visible spectral domain," *Appl. Opt.*, vol. 51, pp. 6259–6267, 2012.

[5] T. Yano and A. Watanabe: "Acoustooptic TeO_2 tunable filter using far-off-axis anisotropic Bragg diffraction," *Appl. Opt.*, vol. 15, pp. 2250-2258, 1976.

[6] J. Champagne, J.-C. Kastelik, and S. Dupont, "Multi-electrode array for spectral bandwidth control," in *Fourteenth School on Acousto-Optics and Applications*, (Torun, Poland), pp.27, Jun 2019.

[7] J. Vanhamel, E. Dekemper, V.B. Voloshinov, E. Neefs, and D. Fussen: "Electrical Bandwidth Testing of an AOTF Transducer as a Function of the Optical Diffraction Efficiency," *J. Opt. Soc. Am. A*, vol. 36, no. 8, pp. 1361–1366, 2019.

[8] K.B. Yushkov, A.I. Chizhikov, O.Y. Makarov, and V.Y. Molchanov: "Linear Phase Design of Piezoelectric Transducers for Acousto-Optic Dispersion Delay Lines Using Differential Evolution for Matching Circuit Optimization," *IEEE Transactions on Ultrasonics, Ferroelectrics, and Frequency Control*, vol. 67, no. 5, pp. 1040–47, 2020.

[9] I. B. Belikov, V. B. Voloshinov, A. B. Kas'yanov, and V. N. Parygin: "Broadband matching of an acouscto-optical-cell transducer using Youla's complex normalization theory," *Radioelektronica*, vol. 31, pp. 30–35, 1988.

[10] A. Goutzoulis and D. Pape, *Design and Fabrication of Acousto-Optic Devices*. New York, Dekker, 1994.

[11] J.S. Beasley and G.M. Miller: *Modern Electronic Communication*. New Jersey: Pearson Prentice Hall, 9th edition, 2008.

[12] J. Vanhamel, E. Dekemper, S. Berkenbosch, and R. Clairquin: "Novel acousto-optical tunable filter (AOTF) based spectropolarimeter for the characterization of auroral emission," *Instrumentation Science & Technology*, vol. 49, no. 3, pp. 245–257, 2021.

[13] J. Vanhamel, S. Berkenbosch, E. Dekemper, P. Leroux, E. Neefs, and E. Van Lil: "Practical Driving Electronics for an AOTF-Based NO_2 Camera," *IEEE Transactions on Instrumentation and Measurement*, vol. 68, no. 3, pp. 874–881, 2019.

[14] E. Dekemper, "Development of an AOTF-based hyperspectral imager for atmospheric remote sensing," Ph.D. dissertation, Fac. of Sci., UCL, Louvain-la-Neuve, Belgium.